Biosensors and Bioelectronics 141 (2019) 111469

Contents lists available at ScienceDirect

Biosensors and Bioelectronics

journal homepage: www.elsevier.com/locate/bios

PAS1-modified optical SIS sensor for highly sensitive and specific detection of toluene

Tran Thi Dung[a,c,1], Ui Jin Lee[a,d,1], Myung Hee Kim[b], Kyoon Eon Kim[d], Hyun Mo Cho[c,e], Cesar D. Fermin[f,g], Dong Hyung Kim[e,*], Moonil Kim[a,c,f,**]

[a] Bionanotechnology Research Center, 125 Gwahangno, Yuseong-Gu, Daejeon, 34141, South Korea
[b] Metabolic Regulation Research Center, Korea Research Institute of Bioscience and Biotechnology (KRIBB), 125 Gwahangno, Yuseong-Gu, Daejeon, 34141, South Korea
[c] KRIBB School, University of Science and Technology (UST), 217 Gajeongno, Yuseong-Gu, Daejeon, 34113, South Korea
[d] Department of Biochemistry, College of Natural Sciences, Chungnam National University, 99 Daehangno, Yuseong-Gu, Daejeon, 34134, South Korea
[e] Division of Advanced Instrumentation Institute, Korea Research Institute of Standards and Science (KRISS), 267 Gajeongno, Yuseong-Gu, Daejeon, 34113, South Korea
[f] Department of Biology, College of Arts & Sciences, Tuskegee University, 36088, USA
[g] Ministerio de Salud Publica (MSP) & Caribbean Biotechnology Labs (CBL), Santo Domingo, DN, the Dominican Republic

ARTICLE INFO

Keywords:
Bio-receptor
PAS1
Solution immersed silicon
Ellipsometry
Toluene

ABSTRACT

We report on a novel solution immersed silicon (SIS) sensor modified with bio-receptor to detect toluene. To perform this approach, bio-receptor PAS1 which specifically interacts with toluene was chosen as a capture agent for SIS ellipsometric sensing. We constructed wild PAS1 and mutant PAS1 (F46A and F79Y) which are toluene binding-defective. Especially, we utilized an easily accessible capturing approach based on silica binding peptide (SBP) for direct immobilization of PAS1 on the SiO_2 surfaces. After the immobilization of SBP-tagged PAS1 to the sensing layers, PAS1-based SIS sensor was evaluated for its ability to recognize toluene. As a result, a significant up-shift in Psi (Ψ) was clearly observed with a low limit of detection (LOD) of 0.1 μM, when treated with toluene on wild PAS1-surface, but not on mutant PAS1-sensing layers, indicating the selective interactions between PAS1 and toluene molecule. The PAS1-SIS sensor showed no changes in Psi (Ψ), if any, negligible, when exposed to benzene, phenol, xylene and 4-nitrophenol as negative controls, thereby demonstrating the specificity of interaction between PAS1 and toluene. Taken together, our results strongly indicate that PAS1-modified ellipsometry sensor can provide a high fidelity system for the accurate and selective detection of toluene.

1. Introduction

Toluene is one of the representative water pollutants (Karaconji et al., 2006) that can be found in natural waters as aromatic hydrocarbons. These environmental pollutants can contaminate water quality. This toxic organic compound has been reported to cause irritation symptoms (Shinohara et al., 2004) in the respiratory tract, skin, eyes, and cause fatigue, headache and dizziness, and serious health problems such as heart arrhythmia, central nervous system disorders, and so on. The National Environmental Drinking Water Regulations (NPDWR) of the US Environmental Protection Agency (EPA) limit the maximum concentration of toluene in drinking water to 1 ppm to protect public health, because toluene has potential to cause serious pollution problem on surface water and drinking water (WHO, 2011; USEPA, 2009).

To date, gas chromatography (GC) (Jurdáková et al., 2008) or gas chromatography mass spectrometry (GC-MS) (Cacho et al., 2016), solid phase extraction (SPE) (M. Meney and M. Davidson, 1998) and solid phase microextraction (SPME) (Nojavan and Yazdanpanah, 2017) techniques have been widely used to identify toluene in liquid phase. However, this technique has the drawback of requiring additional preconcentration processes for a long time to analyze chemicals from contaminated water (Campillo et al., 2004; Goedecke et al., 2017). A technology for detecting aromatic hydrocarbons in industrial cooling water based on flame ionic detectors (Olatunji et al., 2014) and fluorescence (Mirnaghi et al., 2019) has been developed. This technology can effectively detect organic compounds in liquid, but requires expensive measuring equipment. Fiber optic chemical sensors have been reported to measure toluene in liquid sample (Wolfbeis, 2002). These sensors are advantageous in that they can be miniaturized for field

* Corresponding author.
** Corresponding author. Bionanotechnology Research Center, 125 Gwahangno, Yuseong-Gu, Daejeon, 34141, South Korea.
E-mail addresses: donghyung.kim@kriss.re.kr (D.H. Kim), kimm@kribb.re.kr (M. Kim).
[1] These authors contributed equally to this work.

https://doi.org/10.1016/j.bios.2019.111469
Received 10 April 2019; Received in revised form 18 June 2019; Accepted 22 June 2019
Available online 26 June 2019
0956-5663/

applications, but have disadvantages such as toxic and fragile materials. Recently, a carbon nanotube-based CNTFET sensor system coupled to gas chromatography has been reported for aromatic hydrocarbons detection (Silva et al., 2009). The FET type sensor has the advantage of high sensitivity, but the manufacturing process of the device is complicated and expensive facilities are required. Surface plasmon resonance (SPR) has been used as one of the most commonly used optical sensors for analyzing biomolecular interactions (Dung et al., 2018). It can provide superior analytical performance with respect to sensitive measurements and fast response with label-free, real-time monitoring technique using the chip coated with a thin gold layer (Nguyen et al., 2015; Kim et al., 2017). The SPR analysis, however, needs to separate the bulk signals induced by a thermal noise phenomena and a refractive index changes of surrounding medium (Xiao et al., 2010; Kim et al., 2014; Liu et al., 2015). Therefore, there is a need for a highly sensitive measurement system that is simple to use, reliable, and economical for low molecular weight toxic organic compounds. Recently, a silicon based SIS sensor platform has been developed based on the principle that signals can be amplified without using a gold film of a conventional SPR sensor by using a single-wavelength ellipsometry technique at a specific incident angle at which *p*-polarized light with negligible reflectance at the silicon surface (Diware et al., 2017a). The SIS sensor can measure two ellipsometric parameters (Ψ and Δ) simultaneously at a single sensing point. Ψ is highly sensitive to the thickness changes via biochemical interactions on the silicon surface and Δ represents the refractive index variations of the medium (Diware et al., 2015, 2017b). The biosensor has several advantages for the limitations of measurement errors and the enhancement of analytical performance as follows. First, the silicon chip can provide superior flatness enabling an increase of the biosensing reproducibility. Second, the SIS signals are specific to the thickness variations of the chip regardless of the refractive index changes of surrounding environments at Brewster angle (Diware et al., 2015). In addition, SIS sensor technology can manufacture a sensor chip at a very low cost by using silicon as a substrate material, and can be used as a measuring device in various fields such as disease diagnosis, food, and environmental micro-toxin measurement requiring reliable measurement.

Toluene is an important ligand for the activation of TodS/TodT signaling in *Pseudomonas putida* (Koh et al., 2016). The TodS protein has a toluene-binding domain, PAS1. Because of the toluene adsorption capacity of PAS1, the TodS protein has been applied to the biological purification of toluene. It is well known that PAS1 binding of toluene can cause autophosphorylation and structural changes of TodS in TodS (Lacal et al., 2006). Based on a strong, stable interaction mechanism between PAS1 and toluene, PAS1 has the potential to be used as a biological recognition element for toluene detection. In this study, we developed a receptor-based high sensitivity SIS sensor system capable of detecting toluene in liquid by using PAS1 protein which selectively complexes with toluene among a wide range of aromatic hydrocarbons. This sensor demonstrated detection limit of 0.1 μM and excellent selectivity for toluene molecule, indicating that it can be useful in industrial applications to facilitate low molecule screening and water pollution monitoring.

2. Materials and methods

2.1. Materials, strains, vectors, and enzymes

Toluene, phenol, O-xylene, benzene and 4-nitrophenol were purchased from Sigma-Aldrich and used without further purification. *E. coli* strian DH5α was used as host for subcloning and *E. coli* BL21 (DE3) (Novagen, WI) for gene expression. pGEM T-easy vector (Promega, WI) was used as vector for sub-cloning and amplification of full-length gene, and pET-21a (+) (Novagen, WI) was used as vector for expression of PAS1 domain and its mutants. All the restriction enzymes and modifying enzymes were purchased from Takara (Japan) and used according to the recommendations of supplier. A preparation of vector DNA was carried out using QIAEX II gel extraction kit (Qiagen, Germany). Silicon wafer (100) as the SIS sensor chip was purchased from MCL Electronics Materials (China), and 11.5 x 11.5 mm sensor chips were used for this work.

2.2. Gene cloning, expression of recombinant fusion protein, and purification

In order to clone the SBP-PAS1 fusion gene, the partial gene encoding for the PAS1 domain of TodS in *Pseudomonas putida* was amplified with the 5′ primer (ATC CAT ATG CAT ACC AAA CAT AGC CAT ACC AGC CCG CCG CCG CTG GGA GGA TCA GGA GGA TCA GGA GGA TCA GGA GGA TCA AAG GAG AAA GGA TCT GAA) and the 3′ primer (CAA CTC GAG CTC CAA TTC CTG GTT CTT), via PCR. The resultant DNA fragment was then inserted into the pET-21a (+) plasmid using the NdeI/XhoI restriction enzyme cleavage sites. For the cloning of the mutant PAS1 fusion genes (SBP–F46A and SBP- F79Y), overlap extension PCR was performed with flanking primers (forward primer: ATC CAT ATG CAT ACC AAA CAT AGC/reverse primer: CAA CTC GAG CTC CAA TTC CTG GTT CTT) on either end of the template and internal primers (F46A forward primer: 5′- GCT GTG GGC CTT CTT GAT GCT-3'/F46A reverse primer: AGC CTC GTA GAG CCC ATC AAA/F79Y forward primer: GCC TGG AAG GCG CGT TGG TGG/F79Y reverse primer: GGC TGG CTT CCC TCG TAT TTC) that contain the base changes of interest and bind to the region where the replacement will occur. The resultant PCR products were then inserted into the pET-21a (+) plasmid using the NdeI/XhoI sites. Recombinant protein expression was performed as described previously (Koh et al., 2016). Briefly, plasmids were transferred to expression host, *E. coli* BL21 (DE3) (Stratagen, CA) and plated on LB (Luria Bertani) plates. A single colony from a fresh plate was picked and grown at 37 °C in 3 ml of Luria-Bertani broth, LB, containing 100 mg/ml ampicillin until OD_{600} = 0.6. They were inoculated in 100 ml of LB with ampicillin. Cells were grown at 37 °C with shaking until OD_{600} = 0.6. Cells were induced with 1 mM isopropyl-2-D-thiogalactopyranoside (IPTG) (GibcoBRL, NY) and grown for 4 h. Cells were then harvested by centrifugation at 6,000 g at 4 °C for 10 min. Harvested cells were resuspended in 50 mM Tris-HCl buffer (pH 8.0), and disrupted by sonication. The crude cell lysates were separated into total, soluble, and insoluble fractions, which were analyzed by 12% SDS-PAGE. In order to purify the recombinant proteins, 10 ml of the crude cell lysates were loaded onto an IDA-miniexcellose affinity column (Bioprogen, Korea). The recombinant proteins were subsequently eluted with 5 mL of 0.5 M imidazole in the same buffer (50 mM phosphate, 0.5 N NaCl, pH 8.0). The purified protein then dialyzed against phosphate-buffered saline (PBS, pH 7.4) overnight at 4 °C. The dialyzed proteins were further purified by size exclusion chromatography (SEC) using a Superdex G75 column (GE Healthcare, UT). The protein concentration was determined by Nano drop (Thermo scientific, MA). Finally, all recombinant proteins were concentrated to 5 mg/ml, and stored in −80 °C for further experiments.

2.3. On-chip fluorescence imaging analysis

On-chip fluorescence analysis was performed as described previously (Nguyen et al., 2018). Briefly, each purified SBP-tagged protein G was prepared at a concentration of 100 μg/ml, spotted on a slide glass chip for 30 min at 4 °C, and then washed with PBST (10 mM PBS buffer, 0.005% Tween 20, pH 7.4) and deionized water. The glass chips were then incubated with anti-chlorine IgG (whole molecule) in FITC (1: 40000) for 1 h at 4 °C, washed with PBST and deionized water and finally dried with nitrogen gas. The fluorescence images were obtained using GenePix 4200 A Array Scanner from Axon Instrument Inc. (Union City, CA). The PMT power was 70%, and the excitation wavelength was 532 nm. The intensity values were calculated by Multi Gauge Ver3.0 program.

2.4. Atomic force microscopy (AFM) analysis

For the AFM analysis, SBP-tagged PAS1 (5 mg/ml in a PBS buffer, pH 7.4) was dried on top of the SiO_2 surfaces, and scanned with a multimode with Nanoscope V controller. AFM images were obtained in the tapping mode under ambient conditions using the Igor Pro 6.36 program. The height and the roughness were determined from horizontal line scans (n = 3 for each crater, 3 craters/sample).

2.5. SIS measurement for toluene detection

The PAS1-SIS toluene sensor system used a p-type silicon wafer (100) cut to 11.5 × 11.5 mm as a sensor chip, which was cleaned with absolute ethanol for 30 min before being applied to the sensor cell tilted of 2° to the prism surface. The PBS was allowed to flow for about 2–5 min until the sensor signal stabilized. The incident angle of probing light was automatically adjusted at the Brewster angle with respect to the sensor chip by using goniometer (Huber Corp.) mount on SIS system which can provide a high accuracy of 0.001°. Since the silica binding peptide is fused to PAS1, one ml of the PAS1 protein solution was directly added into the two channels of the SIS sensor system without any surface modification treatment, and immobilized in such a manner that the orientation was controlled. One hundred ug/ml of PAS1 protein (PBS, pH 7.4) was prepared and utilized in this study, as optimized in our previous study, and the flow rate was 60 µl/min. The sensor layer was washed thoroughly with PBS solution to remove unbound or weakly bound proteins on the surface. The result of the interaction between toluene and PAS1 is measured by varying the ellipsometric surface thickness.

3. Results and discussion

3.1. Rationale for PAS1-SIS-based toluene sensor

Herein, the optical sensor used as the new detection system is an elliptically polarized SIS sensor. The system uses two surface sensitivity parameters elliptical polarization angle (Ψ, Δ). The ellipsometric constants (Ψ, Δ) representing the change in polarization state in the SIS system indicate the degree of amplitude and phase variation, respectively from linearly polarized light of incident beam (Diware et al., 2017a). Ψ is highly sensitive to thickness changes of silicon surface and Δ maintains virtually constant values regardless of surrounding conditions at non-reflection condition of p-polarized wave as Brewster angle (Diware et al., 2015, 2017b). The robust signals of SIS sensor were obtained by detecting Ψ for thickness variations of the surface with biochemical reactions on the chip. As shown in Fig. 1, the SIS system consists of a light source, a fixed polarizer, an SIS sensor assembly, a rotation analyzer and a detector. The incident light (532 nm wavelength) polarized linearly of within 2° by the polarizer is reflected to the sensor by a prism that bends the incident and reflected beam close to Brewster angle (72.185°) (Diware et al., 2017a). The polarization angle with respect to the plane of incidence was provided closely to the Ψ values of SIS to analyze the normalized intensity by Fourier transform. It is available to overcome experimental errors employed by a nonlinearity and gain variations of detector. The SIS chip was combined by tilting 2° to prism surface, resulting in enhancement of signal-to-noise (S/N) ratio by eliminating the noise signals via reflected beam to prism surface (Diware et al., 2015). The sensitivity of previous SPR detection was achieved in the p-ware anti reflection mode with a gold film substrate (Abbas et al., 2011). However, change in the refraction index can be affected by the buffer solution as well as the thickness of the film, an important limitation of the use of SPR (Drescher et al., 2009; Shumaker-Parry and Campbell, 2004). However, it is difficult to measure the signal of 5×10^{-5} RIU or more due to the refractive index change due signals also collected from the surrounding surfaces or high refractive index of materials such as DMSO when used as the solvent adding noise to the target signal (Maisonneuve et al., 2011; Phan et al., 2016). It is difficult to measure a reliable and noise free signal when the surfaces surrounding the target signal contaminate the measurements. Yet, even though the SIS system is similar to the SPR method in signal amplification under p-wave anti-reflex condition, when the buffer solution is used for the incident medium, the refractive index change does not affect the target signal, resulting in high sensitivity and robust signals (Diware et al., 2015, 2017a, 2017b). The above condition allows measuring only changes in pure bio-membrane without being influenced by the surrounding environment, and has an advantage that it can be applied to the search for low molecular weight and low concentration substances. In this study, we developed a novel high sensitivity SIS sensor modified with a ligand-specific bio-receptor to specifically detect low molecular substances such as toluene. In particular, we adopted PAS1, a high affinity binding protein to toluene, as a sensing element to sensitively and selectively identify the target analyte. The excellent selectivity, high S/N ratio and cost effectiveness of the PAS1-based SIS sensor will gain insight into screening of low molecular substances.

3.2. Selection of silica binding peptide (SBP)

The technique of effectively anchoring the capture agent to the SiO_2 surface is required for developing a sensitive SIS sensor. In order to

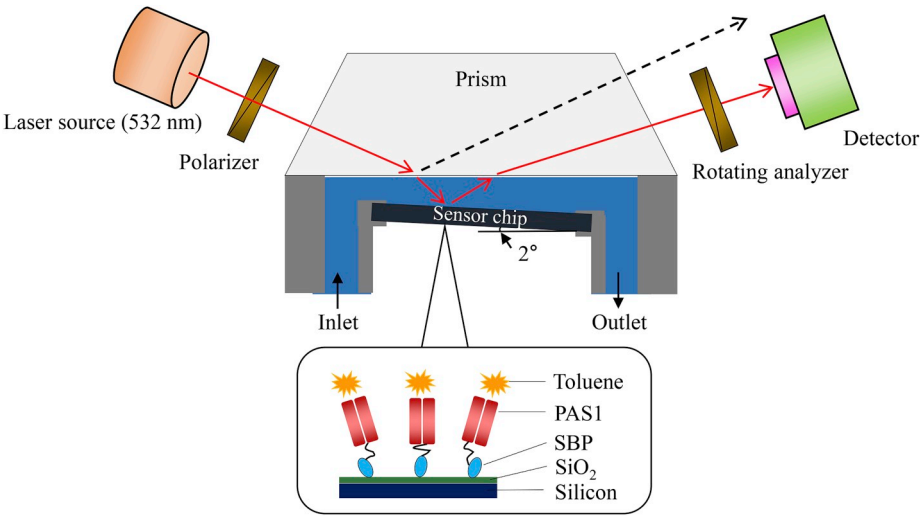

Fig. 1. Schematic diagram of PAS1-based SIS sensor for toluene detection. The SIS system consists of a light source, a fixed polarizer, an SIS sensor assembly, a rotation analyzer and a detector. The incident light (532 nm wavelength) is reflected to the sensor by a prism that bends the incident and reflected beam close to Brewster angle (72.185°).

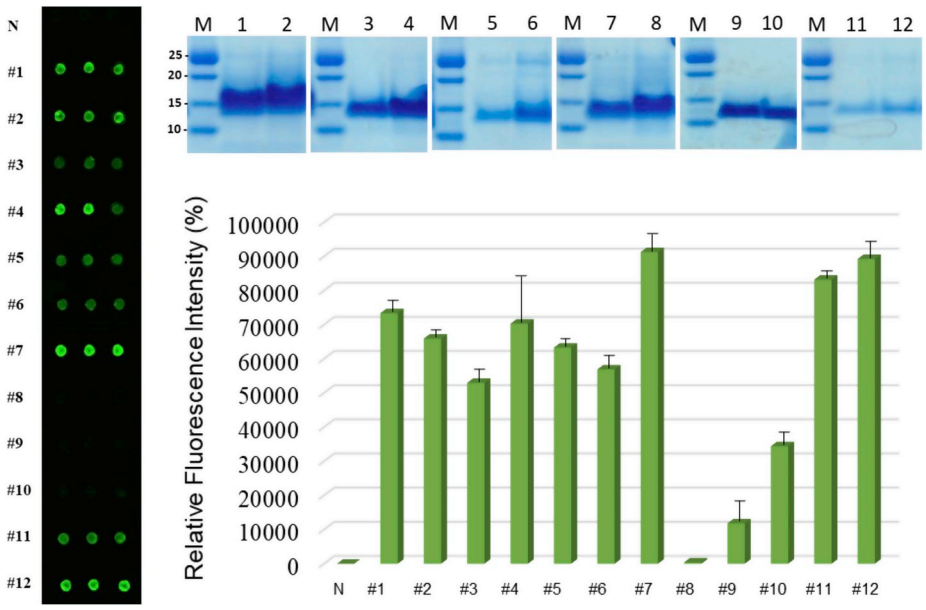

Fig. 2. Fluorescence measurement of FITC-labeled IgG onto SBP-fused protein G deposited on the SiO_2 surface. SDS-PAGE analysis of the recombinant protein Gs fused with 12 different sequences of SBP (Upper panel). Fluorescence of the proteins was quantified using the GenePix Pro 6.0 system (Axon Instruments, CA). Relative fluorescence signal-intensities (%) were graphed (Lower panel). SBP #1, MSPHPHPRHHHT; #2, RLNPPSQMDPPF; #3, HPPMNASHPHMH; #4, CHKKPSKSC; #5, MRKLPDAPGMHTW; #6, MRALPDA; #7, RGRRRRLSCRLL; #8, QTWPPPLWFSTS; #9, HTKHSHTSPPPL; #10, KSLSRHDHIHHH; #11, MRKLPDA; #12, AFILPTG.

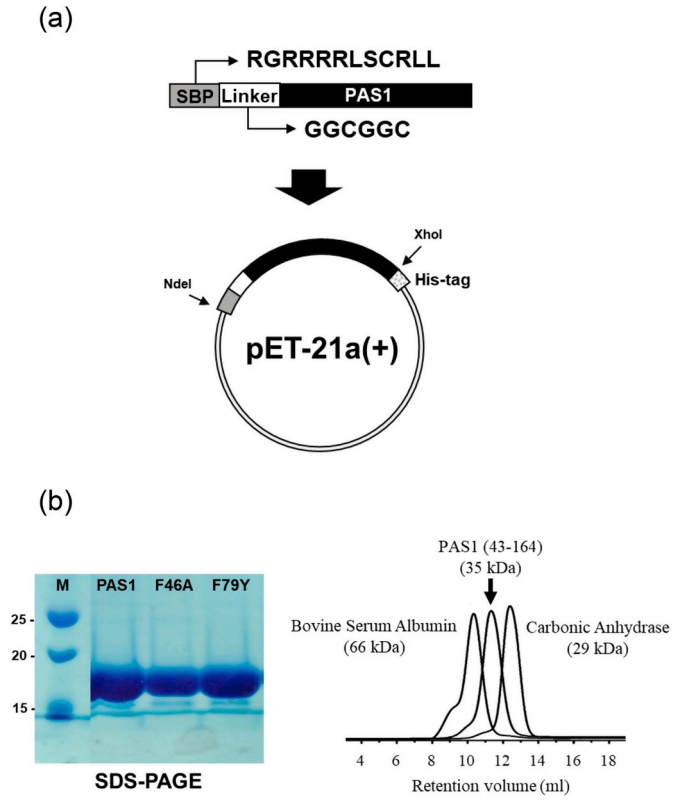

Fig. 3. Construction of the pET-21a (+)-PAS1 vector and expression of SBP-tagged PAS1. (a) The map of recombinant plasmid pET-21a (+)-PAS1 for expression of SBP-tagged PAS1. (b) SDS-PAGE analysis of the recombinant SBP-tagged PAS1, F46A and F79Y. SEC analysis of purified SBP-tagged PAS1 (43–164). Eluted PAS1 was compared with the molecular weight standard markers BSA (66 kDa) and carbonic anhydrase (29 kDa).

easily, rapidly, and accurately immobilize PAS1 onto the SIS layer, the SBP with the higher SiO_2 surface affinity was also evaluated. For this purpose, recombinant proteins with 12 different types of SBP fused to protein G were expressed and purified, and then these 12 recombinant proteins were directly immobilized on the surface of the glass slide (Fig. 2). After thorough washing to remove unattached or weakly bound proteins to the surface of the glass slide, the FITC-labeled antibodies were treated to determine the amount of protein G maintained bound to the surface. Fluorescence intensity analysis by fluorescence microscopy was used to select a peptide with the highest binding affinity to the SiO_2 layer. Protein G without SBP was used as a negative control. As shown in Fig. 2, the SBP sequence of RGRRRRLSCRLL showed the strongest fluorescence intensity in our experimental conditions, presumably because of the abundance of basic arginine residues that form iron pairs with siloxide groups on the surface (Marichal et al., 2018). Thus, this amino acids sequence of silica binding moiety was adopted as the functional peptides for silica binding. The map of recombinant pET-21a (+)-PAS1 expression vector was presented in Fig. 3 (a). After IPTG induction, there was an obvious additional band around the molecular weight of 16 kDa, which is consistent with the expected molecular weight of recombinant SBP-PAS1 protein (Fig. 3 (b)).

3.3. Direct immobilization of SBP-PAS1

The PAS1 as capture molecule have specific binding properties to the toluene, which was combined with SBP using gene-cloning methods. The molecule could be directly immobilized to the silicon without any treatments for chemically surface functionalization. It can also provide the PAS1 orientation for increasing the binding efficiency with toluene by anchoring process of SBP on the surface. To apply the sensor chip to toluene detection, PAS1-SBP was injected to the sensing part of SIS biosensor for 3 min, and then washed with PBS buffer to remove the unbound molecules for 1 min. As shown in Fig. 4 (a), the variation of Ψ signal showed approximately 0.4000 by the thickness changes of the chip and the binding level was retained constantly on the washing step. The Ψ value of 0.4000 obtained experimentally corresponds to the thickness of 1.8 nm on the surface, consistent with the estimated molecular size of SBP-PAS1 (16 kDa in MW, 1.8 nm in length).

The SIS surface modified with SBP-PAS1 was imaged through AFM to investigate the homogeneity of the sensor surface of PAS1 which the selected SBP tag was fused to. Fig. 4 (b) shows an AFM 3D image of PAS1 (100 mg/ml) demonstrating the binding of the protein of interest on the SIS surface. Software for AFM (Dimension 3100, Veeco Inc.) software was used to calculate the average surface roughness of each AFM image. The mean coverage of the exposed bare surface was set to 0%, and PAS1 without SBP was evaluated as a negative control. The average coverage of SBP-PAS1 on the SiO_2 surface of SIS was measured

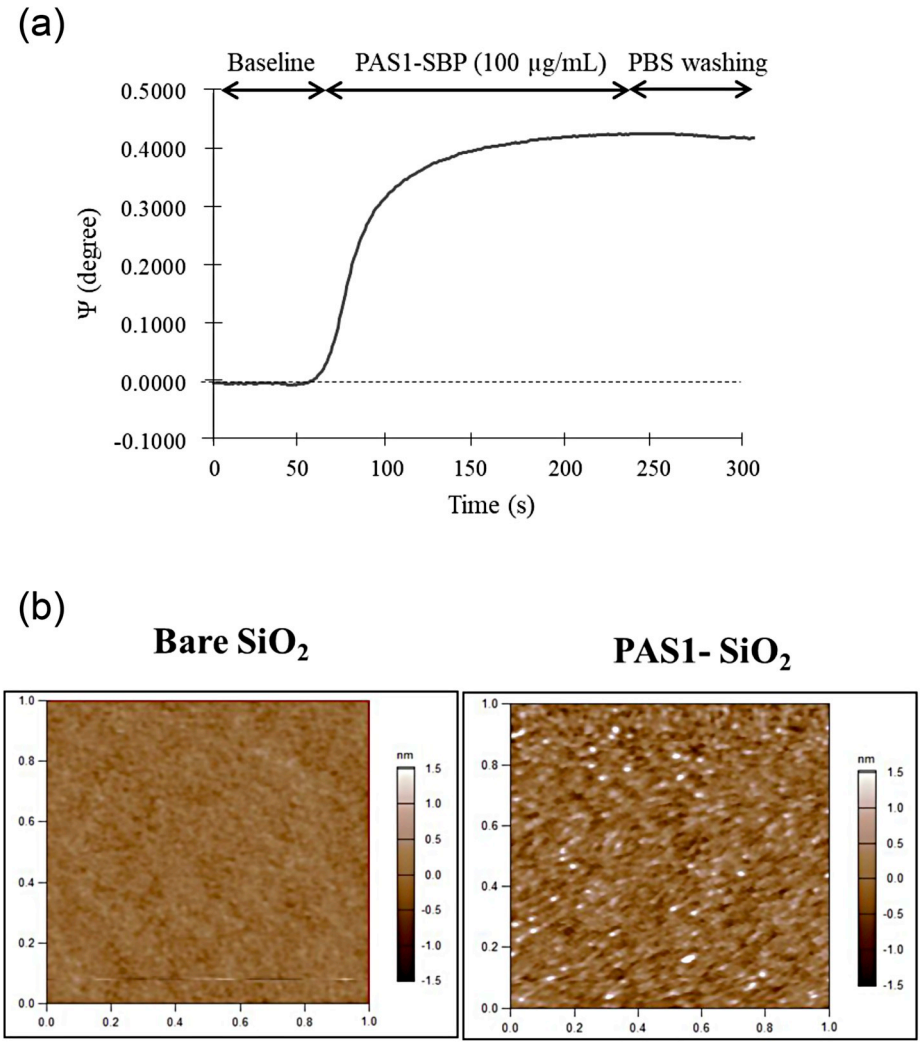

Fig. 4. Direct immobilization of SBP-PAS1 on the SIS sensor chip. (a) Thickness of SBP-PAS1 layer measured by SIS ellipsometry. (b) AFM images of SBP-tagged PAS1 deposited on the SIS silica surface.

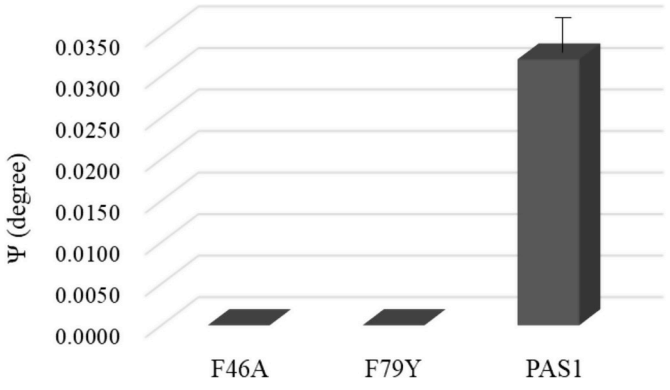

Fig. 5. Mutation analysis of PAS1-modified SIS sensor for toluene detection. SIS analysis shows the interaction of wild PAS1 with toluene, but not mutant PAS1 (F46A and F79Y), which are toluene-binding defective. The SIS signal intensities were expressed in Psi (Ψ).

at 70.4%, while that of SBP-untagged PAS1 was 6.5%, indicating that SBP-PAS1 binds homogeneously and specifically to the SIS surface. In addition, the average thickness of the SBP-PAS1 fusion protein on the silica surface was calculated to be approximately 1.8 nm in agreement with the SIS measurement. This indicates that the SBP-PAS1 fusion protein was immobilized as a single layer having a uniform thickness.

3.4. PAS1-modified SIS analysis for toluene detection

The most important feature of SIS technology is that variation in the surface thickness and change in the refraction index of the surrounding medium can be evaluated at the same sensing point simultaneously (Diware et al., 2015, 2017a, 2017b), leading to sensitive detection of analytes. A detailed SIS measurement is described in Materials and Methods. In the previous studies, F46A and F79Y mutations in PAS1 were found to be defective in toluene binding activity and to block toluene signal transduction pathway. For this reason, the F46A and F79Y mutants were used as negative controls for toluene sensing in this study. F46A is the phenylalanine at position 46 to alanine mutation, and F79Y is the phenylalanine at position 79 to tyrosine mutation. The mutant PAS1 genes were generated through site-directed mutagenesis technique as described in the Materials and Methods section. After expression and purification of PAS1 and mutant PAS1, the corresponding proteins at concentration of 100 µg/ml were applied to the further SIS experiments. Toluene in PBS (100 µM) were injected onto the surface of the SIS sensor functionalized with three different capture agents (PAS1, F46A and F79Y). And then, the interaction behaviors of toluene with wild PAS1 and mutant PAS1 were analyzed using SIS ellipsometry. As shown in Fig. 5, no comparable changes ($\Psi = 0.0010$) in thickness of SIS were observed, when treated with toluene on F46A- or F79Y-modified sensing layer, if any, negligible. However, a significant increase in thickness was measured approximately psi (Ψ) = 0.0350 on

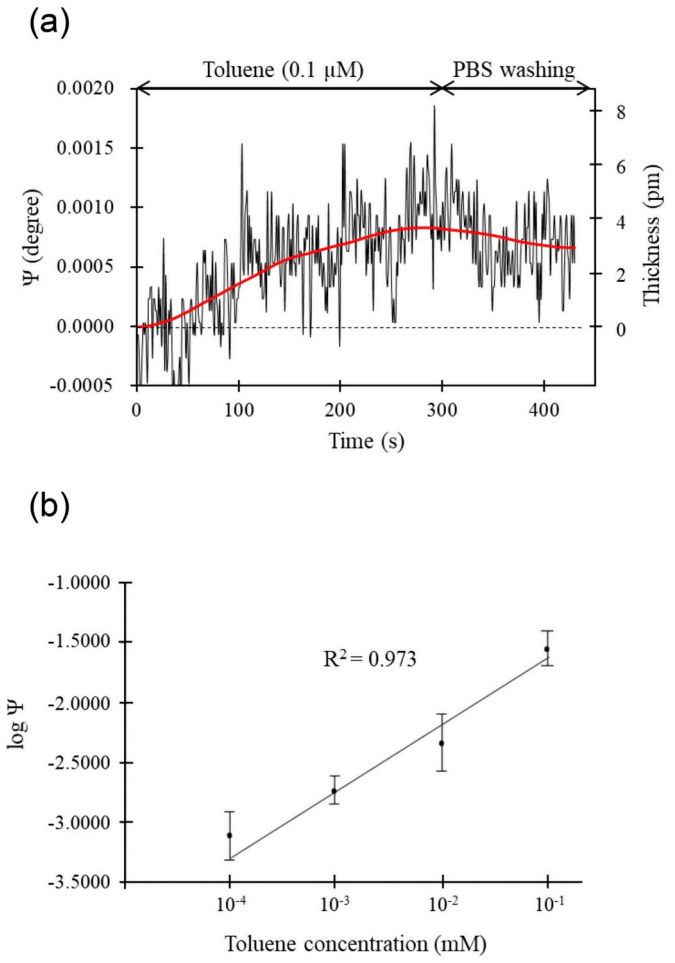

Fig. 6. Sensitivity of PAS1-SIS sensor for toluene detection. (a) SIS profile of lowest measurable concentration of toluene (0.1 μM). (b) Plot of log (Ψ) versus concentration of toluene ranging from 0.1 to 100 μM on the PAS1-modified SIS sensor device.

PAS1-modified surface, which is 35 times higher than that of mutant PAS1 in response to toluene. Given that the SIS response is directly proportional to the amount of toluene interacting with its cognate PAS1 immobilized onto the SiO_2 surface, the changes in SIS signal demonstrated that toluene could bind to PAS1, but not to mutant PAS1.

3.5. Sensitivity for toluene detection

Next, we investigated sensitivity for detection of toluene ranging from 0.1 μM to 100 μM. The corresponding concentrations of toluene were injected onto the PAS1-modified SiO_2 layer at a flow rate of 60 μl/min. The binding signals were treated with an adjacent-averaging method combining a weighted arithmetic mean of the data points. The data-processing algorithm induced a significant pattern of the data, which can measure a definitive value of toluene concentrations in each sample, and then the end-point values of fitted curve were used to establish dose-response curve. Fig. 6 (a) shows the SIS profile of detection limit of anlyte binding. There was a shift in ellipsometric angle ($\Psi = 0.0007$) corresponding to the thickness of 3.1 p.m. in the presence of 0.1 μM of toluene (Diware et al., 2017a), which is less than required current toluene detection standard in drinking water. Fig. 6 (b) shows fitted line plot with a high R-squared ($R^2 = 0.973$, $p < 0.01$) that displays the correlation between toluene concentration and ellipsometric angle (Ψ). The value of Ψ gradually changed with increasing toluene concentration. Our sensor showed the logarithm scale linear dependence in the concentration range of 0.1 μM–100 μM of toluene. For each point of toluene detection, a narrow deviation of the SIS signal was shown, which implies an increase in the reliable SIS signal due to interactions between the PAS1 surface and toluene. In the absence of toluene, no SIS reaction was observed, which means that an increase in the SIS signal is caused by the presence of toluene. The detection limit of 0.1 μM toluene achieved in this study is about 150 times lower than that of the SPR measured in previous studies (Tran and Kim, 2018). To our best knowledge, there is no report that the detection limit of the toluene sensor is below the μM level. Over the past several decades, a variety of techniques for toluene detection have been developed in terms of sensitivity improvement. Washe et al. developed a nanotube-based FET for liquid toluene detection and achieved a detection limit of 23.3 μM (2.1 ppm) (Washe et al., 2010). Burck et al. reported that the polymer clad silica (PCS) fiber-based optical chemical sensor exhibited an LOD of 1.1 μM (0.1 ppm) for toluene in water (Bürck et al., 1998). However, in general, low molecular substances produce relatively low response signals on various sensor surfaces, and thus show a relatively high detection limit. Despite the fact that toluene is a low molecular weight material with a molecular weight of 92.138 Da, achieving a detection limit of 0.1 μM for toluene in this study is due to the use of highly sensitive SIS sensor modified with PAS1, which has an excellent toluene binding affinity. Thus, the results indicate that the PAS1 based SIS detection system can be potentially useful for quantitative detection of toluene in liquid.

3.6. Specificity for toluene detection

In order to accurately assess the presence of toluene, it is necessary to exclude false positive signals from other aromatic hydrocarbons. Therefore, we finally evaluated the specificity of the PAS1-SIS-based toluene detection by comparing the SIS angle change by toluene with that of other benzene compounds including benzene, 4-nitronphenol, O-xylene, and phenol. As shown in Fig. 7, the Ψ value significantly increased ($\Psi = 0.0350$) in response to 100 μM of toluene, while benzene, O-xylene and phenol aromatic hydrocarbons were detected to be negligible. There was a slight shift in the SIS angle ($\Psi = 0.0040$) in the presence of 100 μM of 4-nitronphenol. Recent study by Kuang et al. reported that 4-nitrophenol 2-monooxygenase in *Rhodococcus ruber* was expressed upon toluene stress at the transcript level (Kuang et al., 2018). Thus, it is thought that there might probably be cross reactivity in metabolic pathway of organic tolerance between toluene and 4-nitronphenol. Nevertheless, our results clearly indicate that the SIS sensor incorporating PAS1 has excellent selectivity for toluene. The ability of the sensor to distinguish the target molecule from different analytes is one of the main concerns of chemical sensor development, and is also one of the most difficult problems to solve. To figure out this issue, we have come up with the idea of the use of the PAS1 domain, which has a high affinity to

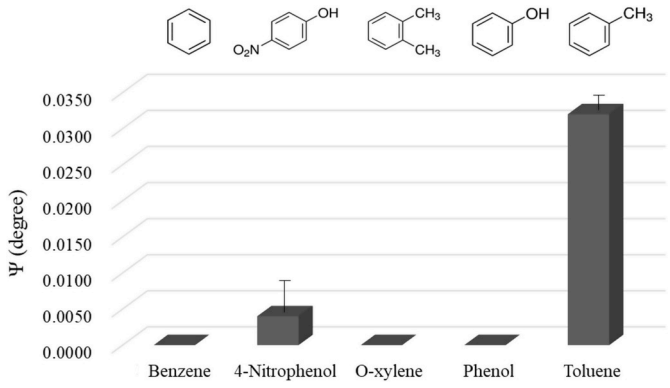

Fig. 7. Specificity of PAS1-SIS sensor for toluene detection over other competing aromatic hydrocarbons such as benzene, 4-nitrophenol, O-xylene and Phenol. The concentration was 100 μM for all analytes examined.

toluene. Despite the excellent selectivity of bio-capture agents, the biggest limitation of bio-receptor-based sensors is stability (Nguyen et al., 2019). Recently, an interesting studies on stability of sensors based on bioreceptor has been published. Park et al. reported that the bioreceptor-based graphene FET sensor exhibited outstanding stability as approximately 95% activity was maintained for 10 days at room temperature (Park et al., 2012). Lee et al. showed that more than 60% sensitivity of polypyrrole nanotubes functionalized with a bioreceptor was maintained for 10 weeks when stored at 25 °C even in air-dried conditions (Lee et al., 2012). Along this line, research aiming at the development of SIS devices for improving temperature and long-term stability is further required.

4. Conclusions

The purpose of this study was to evaluate the performance of bio-SIS sensors for the selective detection of low molecular weight substances with low detection limit. Aromatic hydrocarbon toluene of 92.138 Da was adopted as a model compound of small molecule and toluene binding domain PAS1 was used as a capture agent for toluene. The toluene sensing element PAS1 was immobilized on the surface of SIS silicon in a controlled orientation by means of functional peptides self-assemble on silica through the silica binding moiety. The SIS sensors are advantageous for detection of small and low concentration compounds, and are cost-effective non-labeling optical sensors because they use inexpensive silicon instead of gold films. When the sensor is exposed to a liquid toluene sample, toluene is affinity bound to PAS1 on the sensor surface, and quantitative and qualitative analysis is performed by measuring the optical thickness change due to the adsorption of toluene. The SIS toluene sensor coated with recombinant PAS1 expressed in *E. coli* showed logarithm scale linear dependence in the concentration range of 0.1 μM–100 μM of toluene. In particular, the detection limit of 0.1 μM (0.009 ppm) for toluene is almost 1,000-fold lower than the maximum concentration level (8.24 ppm) found in the samples around the oil spill (Fraker, 2013). Thus, our sensor can be used in applications requiring higher sensitivity, such as drinking water testing requiring detection limits of about 0.5–1 ppm (Demir and Ergin, 2013; WHO, 2011; Mandinic et al., 2010). Also, due to the inherent specificity of PAS1, the sensor exhibited excellent selectivity for toluene. Therefore, our results show that PAS1-SIS sensor can potentially be applied to the monitoring and analysis of water pollutants, and is also applicable to low molecular substance screening applications.

CRediT authorship contribution statement

Tran Thi Dung: Conceptualization, Formal analysis, Writing - original draft. **Ui Jin Lee:** Conceptualization, Writing - original draft. **Myung Hee Kim:** Writing - original draft. **Kyoon Eon Kim:** Conceptualization. **Hyun Mo Cho:** Formal analysis. **Cesar D. Fermin:** Writing - original draft. **Dong Hyung Kim:** Formal analysis. **Moonil Kim:** Conceptualization, Formal analysis.

Acknowledegments

This work was equally supported by the BionNano Health-Guard Research Center as Global Frontier Project (H-GUARD 2013M3A6B2078950) and the Korea Research Institute of Bioscience and Biotechnology Initiative Research Program.

References

Abbas, A., Linman, M.J., Cheng, Q., 2011. Biosens. Bioelectron. 26 (5), 1815–1824.
Bürck, J., Mensch, M., Krämer, K., 1998. Field experiments with a portable fiber-optic sensor system for monitoring hydrocarbons in water. Field Anal. Chem. Technol. 2 (4), 205–219.
Cacho, J.I., Campillo, N., Viñas, P., Hernández-Córdoba, M., 2016. RSC Adv. 6 (25), 20886–20891.
Campillo, N., Aguinaga, N., Vinas, P., Lopez-Garcia, I., Hernandez-Cordoba, M., 2004. J. Chromatogr., A 1061 (1), 85–91.
Demir, V., Ergin, S., 2013. J. Chem. 6 2013.
Diware, M.S., Cho, H.M., Chegal, W., Cho, Y.J., Jo, J.H., O, S.W., Paek, S.H., Yoon, Y.H., Kim, D., 2015. Analyst 140 (3), 706–709.
Diware, M.S., Cho, H.M., Chegal, W., Cho, Y.J., Kim, D.S., O, S.W., Kim, K.S., Paek, S.H., 2017a. Biosens. Bioelectron. 87, 242–248.
Diware, M.S., Cho, H.M., Chegal, W., Cho, Y.J., O, S.W., Paek, S.H., Kim, D.S., Kim, K.S., Min, Y.G., Jo, J.H., Shin, C., 2017b. Biointerphases 12 (1), 01A402.
Drescher, D.G., Ramakrishnan, N.A., Drescher, M.J., 2009. Methods Mol. Biol. 493, 323–343.
Dung, T.T., Oh, Y., Choi, S.J., Kim, I.D., Oh, M.K., Kim, M., 2018. Sensors 18, 103.
Fraker, M.A., 2013. Hum. Ecol. Risk Assess. 19 (1), 28–52.
Goedecke, C., Fettig, I., Piechotta, C., Philipp, R., Geissen, S.U., 2017. Anal. Methods 9 (10), 1580–1584.
Jurdáková, H., Kubinec, R., Jurčišinová, M., Krkošová, Ž., Blaško, J., Ostrovský, I., Soják, L., Berezkin, V.G., 2008. J. Chromatogr., A 1194 (2), 161–164.
Karaconji, B., Skender, L., Karacic, V., 2006. Bull. Environ. Contam. Toxicol. 76 (3), 458–462.
Kim, D.H., Cho, I.H., Park, J.N., Paek, S.H., Cho, H.M., Paek, S.H., 2017. Biosens. Bioelectron. 88, 232–239.
Kim, D.H., Seo, S.M., Cho, H.M., Hong, S.J., Lim, D.S., Paek, S.H., 2014. Biosens. Bioelectron. 62, 234–241.
Koh, S., Hwang, J., Guchhait, K., Lee, E.G., Kim, S.Y., Kim, S., Lee, S., Chung, J.M., Jung, H.S., Lee, S.J., Ryu, C.M., Lee, S.G., Oh, T.K., Kwon, O., Kim, M.H., 2016. J. Biol. Chem. 291 (16), 8575–8590.
Kuang, S., Fan, X., Peng, R., 2018. Biotechnol. Biotechnol. Equip. 32 (6), 1418–1430.
Lacal, J., Busch, A., Guazzaroni, M.E., Krell, T., Ramos, J.L., 2006. Proc. Natl. Acad. Sci. Unit. States Am. 103 (21), 8191–8196.
Lee, S.H., Kwon, O.S., Song, H.S., Park, S.J., Sung, J.H., Jang, J., Park, T.H., 2012. Biomaterials 33 (6), 1722–1729.
Liu, Y., Liu, Q., Chen, S., Cheng, F., Wang, H., Peng, W., 2015. Sci. Rep. 5, 12864.
M. Meney, K., M. Davidson, C., 1998. Analyst 123 (2), 195–200.
Maisonneuve, M., Song, I.-H., Patskovsky, S., Meunier, M., 2011. Optic Express 19 (8), 7410–7416.
Mandinic, Z., Curcic, M., Antonijevic, B., Carevic, M., Mandic, J., Djukic-Cosic, D., Lekic, C.P., 2010. Sci. Total Environ. 408 (17), 3507–3512.
Marichal, L., Renault, J.-P., Chédin, S., Lagniel, G., Klein, G., Aude, J.-C., Tellier-Lebegue, C., Armengaud, J., Pin, S., Labarre, J., Boulard, Y., 2018. Langmuir 34 (18), 5312–5322.
Mirnaghi, F.S., Pinchin, N.P., Yang, Z., Hollebone, B.P., Lambert, P., Brown, C.E., 2019. Environ. Sci. Process. Impacts. 21 (3), 413–426.
Nguyen, H.H., Park, J., Kang, S., Kim, M., 2015. Sensors 15, 10481–10510.
Nguyen, H.H., Park, J., Hwang, S., Kwon, O.S., Lee, C.S., Shin, Y.B., Ha, T.H., Kim, M., 2018. Sci. Rep. 8, 337.
Nguyen, H.H., Lee, S.H., Lee, U.J., Fermin, C.D., Kim, M., 2019. Materials 12, 121.
Nojavan, S., Yazdanpanah, M., 2017. J. Chromatogr., A 1525, 51–59.
Olatunji, O.S., Fatoki, O.S., Opeolu, B.O., Ximba, B.J., 2014. Food Chem. 156, 296–300.
Park, S.J., Kwon, O.S., Lee, S.H., Song, H.S., Park, T.H., Jang, J., 2012. Nano Lett. 12 (10), 5082–5090.
Phan, Q.-H., Lo, Y.-L., Huang, C.-L., 2016. Optic Express 24 (12), 12812–12824.
Shinohara, N., Mizukoshi, A., Yanagisawa, Y., 2004. J. Expo. Anal. Environ. Epidemiol. 14 (1), 84–91.
Shumaker-Parry, J.S., Campbell, C.T., 2004. Anal. Chim. 76 (4), 907–917.
Silva, L.I.B., Ferreira, F.D.P., Rocha-Santos, T.A.P., Duarte, A.C., 2009. J. Chromatogr., A 1216 (37), 6517–6521.
Tran, T.-D., Kim, M., 2018. Appl. Sci. Converg. Technol. 27 (6), 184–188.
USEPA, 2009. National Primary Drinking Water Regulations. EPA 816-F-09-004.
Washe, A.P., Macho, S., Crespo, G.A., Rius, F.X., 2010. Anal. Chem. 82 (19), 8106–8112.
WHO: World Health Organization, 2011. Guidelines for Drinking Water Quality, fourth ed. . http://apps.who.int/iris/bitstream/10665/44584/1/9789241548151 eng.pdf.
Wolfbeis, O.S., 2002. Anal. Chem. 74 (12), 2663–2678.
Xiao, X., Gao, Y., Xiang, J., Zhou, F., 2010. Anal. Chim. Acta 676 (1–2), 75–80.